

**General behaviour of the ATLAS solenoid  
magnetic field calculated with the modified  
CERN POISSON package**

**V. I. Klioukhine, B. I. Klochkov**

IHEP, Protvino, Russia

## **Introduction**

To estimate a behaviour of the ATLAS solenoid magnetic field inside the inner tracker volume, hadronic tile calorimeter and solenoid return yoke a set of 2-dimensional calculations is done with the modified CERN POISSON program package [1]. The preliminary results obtained earlier were described elsewhere [2].

The modified POISSON package and new designed interface programs enable to prepare the geometry descriptions of the magnetic systems in a simple way, to increase essentially the number of elements in the magnetic system, to visualize graphically the magnetic field values for different cross-sections of the system, to extract magnetic field map and to use it in the GEANT simulations, to calculate magnetic field integrals for the tracking volume placed into ununiform solenoidal field.

To solve magnetostatic problems for the magnetic systems with the geometry reducing to 2-dimensional case a topology regular triangle mesh is used over all the programs of the package and each node of this mesh is identified by two logical coordinates in the arrays of data and two physical coordinates in the  $xy$ - or  $rz$ -plane in which the geometry of magnetic system is described.

To describe the ATLAS solenoid magnetic system in presence of hadronic tile calorimeter, which consists of the interchanged thin layers of steel and scintillator, the number of the mesh nodes supported by the modified package is increased from 40 000 to 270 000, and the number of regions characterized by the different magnetic properties is enlarged from 60 to 7 000.

The modified POISSON package is installed at AXCERN, ASF, CSF and PARC computer clusters. A calculation of the ATLAS solenoid magnetic system takes about 3 hours of CPU time at the DEC ALPHA machine. At the UNIX machines it is faster.

## Magnetic system description

In present paper we compare the field behaviour for the solenoid magnetic systems with different parameters. In calculations we changed the coil diameter (“small” and “large” coils), coil length of “small” coil, the geometry of the solenoid return yoke and magnetic properties of steel. At this paper we fix the return yoke geometry and use for the B–H dependence in steel a table from [3].

In general, a model of the magnetic system is described as follow (see Figs. 1 and 2, for example):

- The “small” solenoid coils have an inner radius of 1.23 m, a thickness of 1.28 cm, and the lengths of 5.3, 5.8, and 6.3 m. The total currents used for the whole coil lengths are 8.916309, 9.543294, and 10.365991 MA-turnes, that gives magnetic flux density in a center of solenoid equal to 2.0, 1.9817, and 2.0017 T, respectively.

The “large” solenoid coil has an inner radius of 2 m, a thickness of 1.28 cm, and a length of 5.15 m. A total current used for the whole coil length is 9.352670 MA-turnes, that gives magnetic flux density in a center of solenoid equal to 2.0041 T.

- The barrel part of hadronic tile calorimeter has a length of 5.894 m, an inner radius of 2.25 m, an outer radius of 3.81 m and consists of the steel plates and 11 rows of the scintillator plates. The first scintillator row begins from the radius of 2.26 m, and the last one ends at  $r = 3.779$  m, thus there are 1 cm of steel free from scintillator near the inner radius, and 3.1 cm of “free” steel near the outer radius of hadronic calorimeter.

Each odd row of scintillator plates in the barrel part begins and ends at 2.9 cm from each of edges, each even row – at 2.0 cm. Thus, there are 2 cm steel plates at each edge of the barrel part. The thickness of each scintillator plate is 0.4 cm, and the thickness of steel between each two scintillator plates is 1.4 cm. As it is mentioned above, even rows of scintillator plates are shifted along the z-direction over 0.9 cm with respect to the odd ones. There are 325 scintillator plates along each odd row and 326 plates along even row.

A widths of scintillator plates are 9.9,  $2 \times 9.8$ ,  $3 \times 12.8$ ,  $3 \times 14.8$ , and  $2 \times 18.8$  cm. There are 2 mm of “free” steel between the scintillator rows.

- There are two extended barrel parts of hadronic tile calorimeter beginning from the distances of 50 cm from each of edges of the barrel part. Its inner and outer radii are the same as for the barrel part. The length of each extended barrel part is 2.699 m, the inner structure is similar to that one of the barrel part.

Each odd row of scintillator plates in the extended barrel part begins at 2 cm from the side closest to the barrel part and ends at 2.9 cm from the each of edges. Each even row begins at 2.9 cm and ends at 2.0 cm. There are 148 scintillator plates in each row.

- The last part of magnetic system consists of two steel support tubes of 12.3 m length. The first tube has an inner radius of 3.81 m and an outer radius of 3.92 m. In the regions between central and extended barrels this tube has an inner radius of 3.779 m. Thus, its thickness here is not 11 but 14.1 cm and this is important for passing of magnetic flux between central and extended barrels. The second support tube has an inner radius of 4.1 m and a thickness of 10 cm. The gap between these support tubes is filled either with a steel with stacking factor of 0.1778 or with an air, that does not change much the results. For 5.3 and 6.3 m “small” coils this gap is covered with 10 cm steel plate at the edges of extended barrels.

## The behaviour of field podiced by 5.3 m small coil

The general view of the solenoid magnetic system containing “small” coil with a length of 5.3 m is presented in Fig. 1, where the graphic images of the scintillator tiles are removed. Figs. 2-a – 2-c present three enlarged parts of the hadronic calorimeter, where one can see the behaviour of the magnetic flux lines in detail.

Figs. 3–7 show how the value of magnetic flux density and direction of its vector with respect to z-axis are changed as the functions of z and radius (Fig. 6) for different constant values of another coordinate:

- Figs. 3 and 4 present the behaviour of field inside the steel between scintillator plates in central and extended barrels of the tile calorimeter for  $r = 2.3095, 2.51, 2.75, \text{ and } 3.025$  m;
- Fig. 5 displays the field behaviour inside and outside the solenoid return yoke for  $r = 3.85, 4.01, 4.15, \text{ and } 4.3$  m;
- Fig. 6 shows the values of field in the crack between central and extended barrels of the tile calorimeter for  $z = 3.1, 3.2, \text{ and } 3.3$  m;
- Fig. 7 reflects the behaviour of the field inside the inner tracker volume for  $r = 0.0, 0.3, 0.6, \text{ and } 0.9$  m.

In Fig. 8 the double integrals calculated for the real (inhomogeneous) and ideal (homogeneous) solenoid magnetic field inside the inner tracker cavity of 6.8 m length and 1.06 m radius as well as its degradation are shown. The degradation of the real field integral reflects the degradation of the transvers momentum measurements versus pseudorapidity range [4].

From Figs. 3 and 4 one can see that the minimum values of the magnetic flux density inside the steel between the scintillator plates is 0.003–0.006 T. The field inside the solenoid return yoke and in horizontal steel layers between scintillator rows is much higher, but the cross-section of all “free” steel is equal to  $7.4 \text{ m}^2$  that is quite enough to keep an average flux density value in this “free” steel at the level of 1.3 T, assuming the magnetic flux inside the solenoid equal to 9.5 Wb. Figs. 9 and 10 show the field behaviour in the central part of the tile calorimeter barrel in detail.

The value of field inside the scintillator plates presents a special interest. An attempt to estimate such a field gives the minimum value at the level of 0.002–0.005 T in the central region of the scintillator plate.

We calculated also the forces which act to the tile calorimeter supermodules. A half of central barrel and each extended barrel we divided by 3 approximately equal parts in z-direction. The obtained values of radial and axial forces (in tons per radian) together with the dimensions of supermodules are presented in Table 1.

**Table 1**

Forces acting to the tile calorimeter supermodules

$r_{min}$ , m	$r_{max}$ , m	$z_{min}$ , m	$z_{max}$ , m	$F_r$ , t/rad	$F_z$ , t/rad
2.25	4.2	0.000	0.983	-0.130	- 6.080
2.25	4.2	0.983	1.964	-1.484	-18.220
2.25	4.2	1.964	2.947	-5.813	-28.000
2.25	4.2	3.447	4.349	-1.914	- 8.946
2.25	4.2	4.349	5.249	-0.234	- 0.666
2.25	4.2	5.249	6.146	-0.049	- 0.108

## Comparison with large solenoid

Magnetic flux from “large” solenoid coil is 2.6 times larger than from “small” one. The cross-section of “free” steel is not enough to catch this magnetic flux and essential part of the flux lines, as shown in Fig. 11 go through the scintillator rows. It causes the high value of the field in the steel between scintillator plates at the level of 0.1–0.4 T. Due to this reason the field inside scintillator plates is higher too. Some part of magnetic flux goes outside of solenoid return yoke that gives higher fringe field in the region of the muon chambers in comparison with “small” coil.

## Comparison with other small coil lengths

We compare also the behaviour of the magnetic field in the inner tracker volume for different “small” coil lengths [5]. We pay our attention to the angle between the vector of total magnetic flux density and z-axis and to the degradation of the real field integral. For each coil length and for  $r = 0.9$  m

the angle reaches the value of  $25^\circ$  at the end of coil and  $32^\circ$  at the end of inner tracking volume, after that its value stays approximately the same till the end of extended barrel, where it has an essential rise. The degradation of integral at pseudorapidity 1.88 (the corner of the inner tracker volume) is equal to 0.15, 0.19, and 0.24 for 6.3, 5.8, and 5.3 m “small” coil, respectively.

## Toroid field influence

We have studied also how much field is induced in the tile calorimeter and solenoid return yoke by the barrel muon toroid. The muon toroid parameters are taken from [6].

Fig. 12 displays the toroid field distribution in presence of the tile calorimeter. Figs. 13 and 14 show the variation of the magnetic flux density versus the radius and azimuth angle. In these calculations the tile calorimeter is filled with steel with the stacking factor of 0.76. The solenoid return yoke is described in the same way as it was for the solenoid magnetic system. From these pictures one can see that the maximum value of total magnetic flux density induced by toroid in outer tube of the solenoid return yoke is 0.9 T. In the inner support tube and inside the tile calorimeter this value is much less. These values do not effect much on the behaviour of the solenoid field inside the inner tracking volume and slightly influence to the field distribution in the tile calorimeter.

## Conclusions

The proposed model of description of the ATLAS solenoid magnetic system is enough robust and gives satisfied results. The solenoid magnetic field calculated in the region of  $r < 5$  m and  $|z| < 7$  m is extracted into ZEBRA structure file and can be used for further detector simulation with help of specially designed subroutine, which gives space components of magnetic flux density for each entered space point. We are ready to give more complete information to any region of the solenoid magnetic system.

*Acknowledgements.* The authors are thankful to P. Jenni, M. Nessi and A.P. Vorobiev the support of this work and prolific discussions.

## References

- [1] V.I. Klyukhin, B. I. Klochkov, *A Second Life of the CERN POISSON Program Package*. Proc. of the Int. Conf. on the Computing in High Energy Physics, San Francisco, 21-27 April 1994.
- [2] V.I. Klyukhin, B.I. Klochkov, *Preliminary results on the ATLAS solenoid magnetic field calculations in presence of hadronic tile calorimeter*. ATLAS Internal Note TILECAL-NO-007, January, 1994.
- [3] M. Nessi et al., *Computer Models for the TILECAL Magnetic Field Distributions*. ATLAS Internal Note TILECAL-NO-012, May, 1994.
- [4] V.I.Klyukhin, A. Poppleton, J. Schmitz, *Field integrals for the ATLAS tracking volume*. ATLAS Internal Note INDET-NO-023, February, 1993; IHEP Preprint 93-38, Protvino 1993.
- [5] V. Klioukhine, B. Klochkov, M.Nessi, *Applications of the modified CERN POISSON program package to the ATLAS magnetic system simulations*. ATLAS TILE-TR-13, June, 1994.
- [6] W. Kozanecki, Memorandum of 20 July 1994.

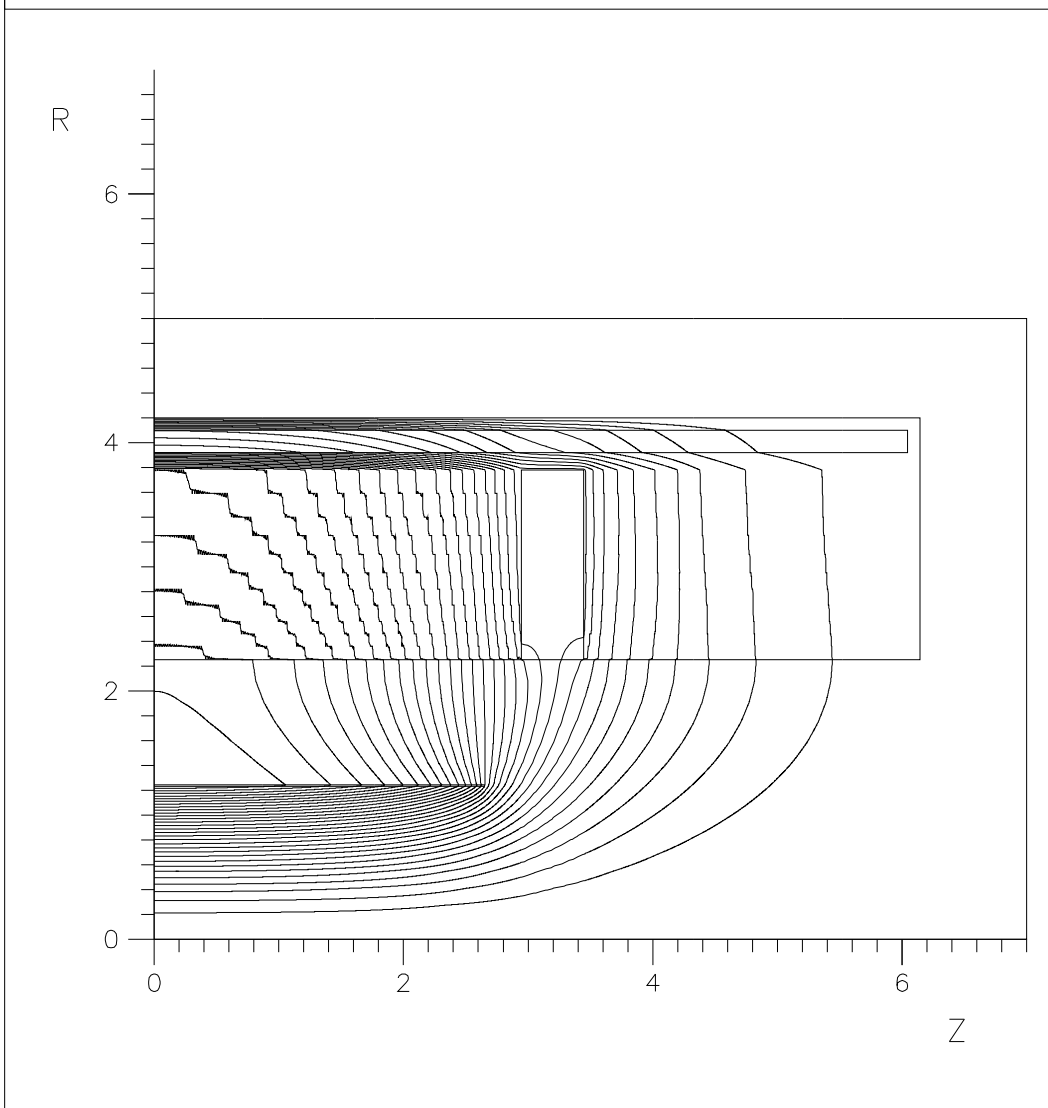


Figure 1. General view of 5.3 m long “small” solenoid magnetic system.



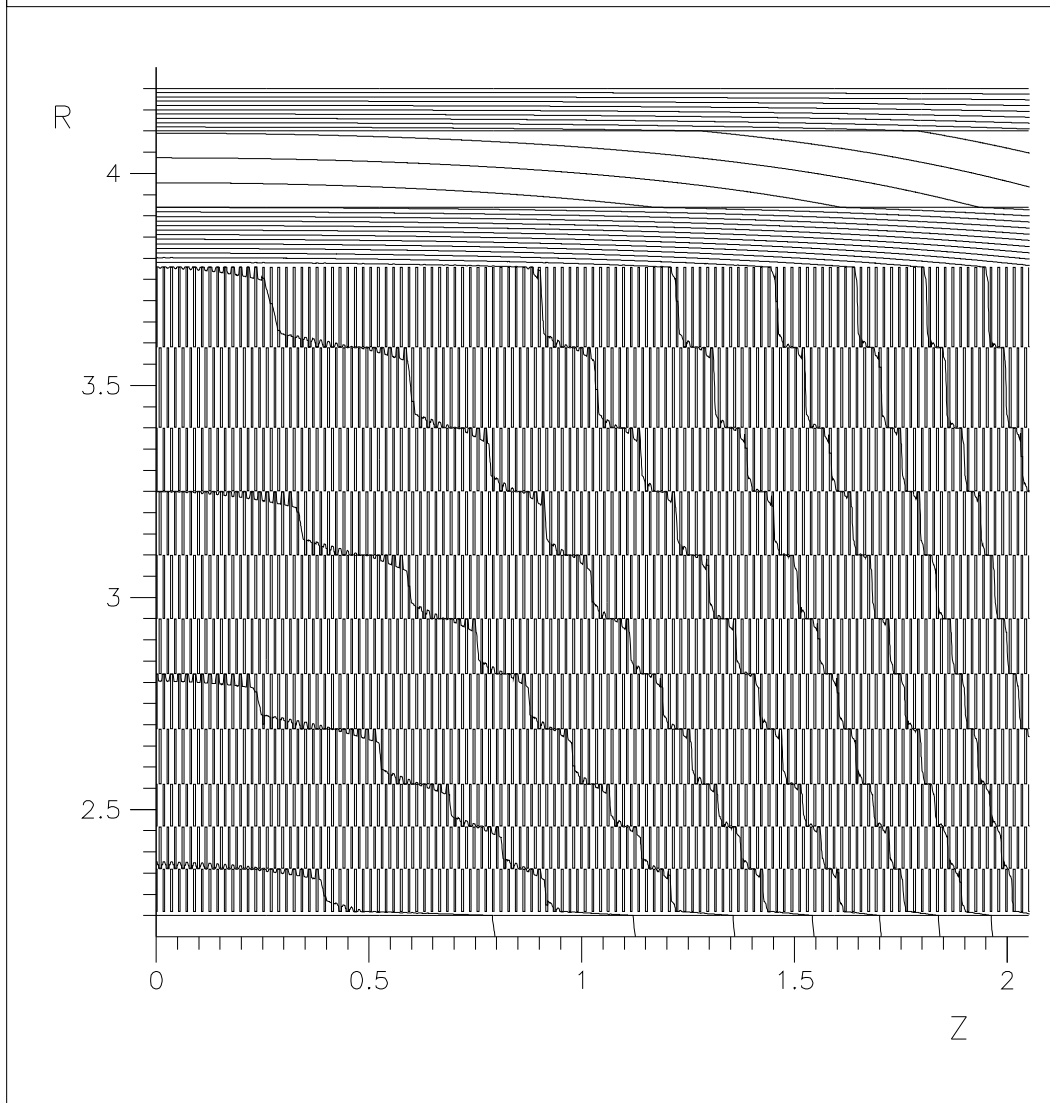


Figure 2-a. Behaviour of the solenoid magnetic field inside the tile calorimeter.

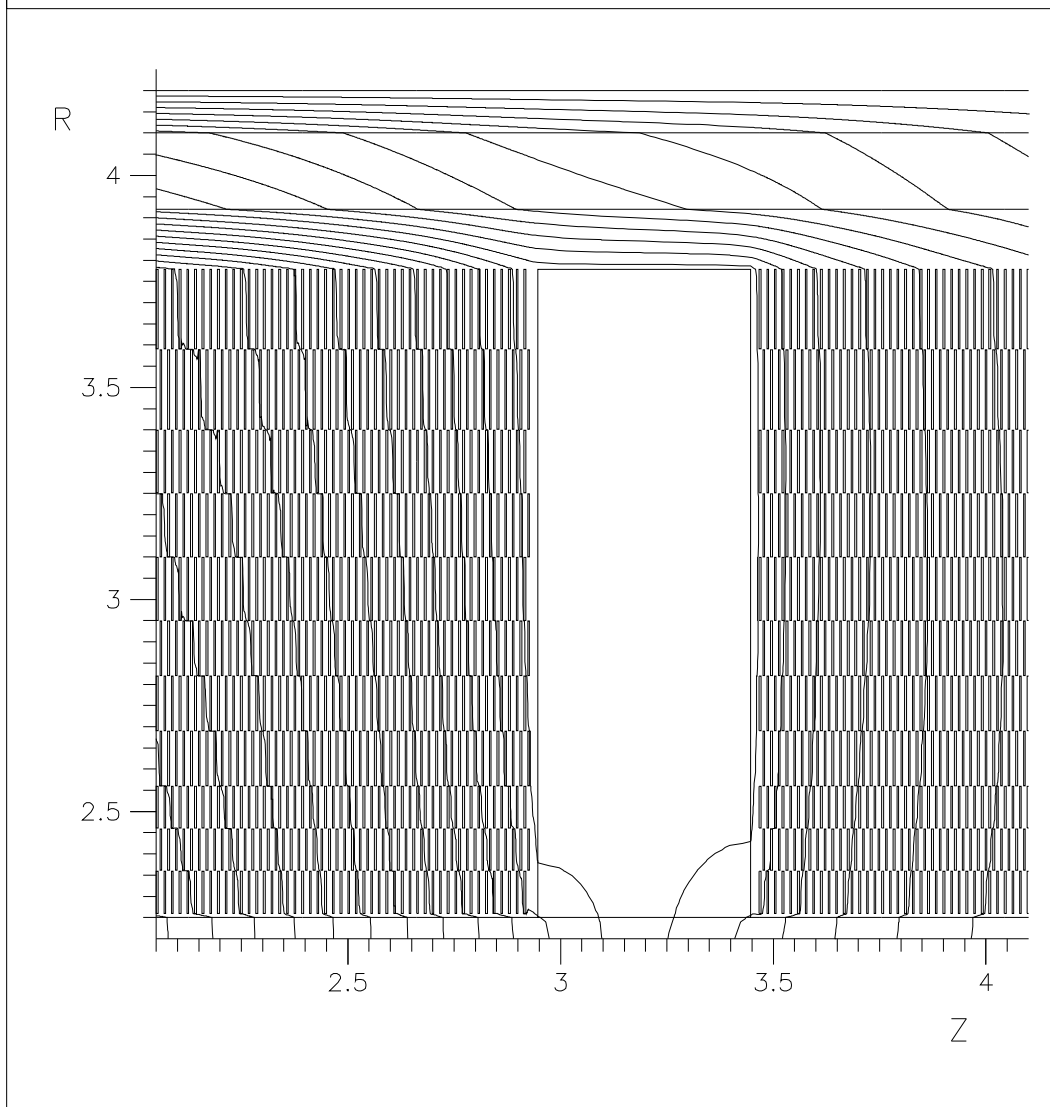


Figure 2-b. Behaviour of the solenoid magnetic field inside the tile calorimeter.

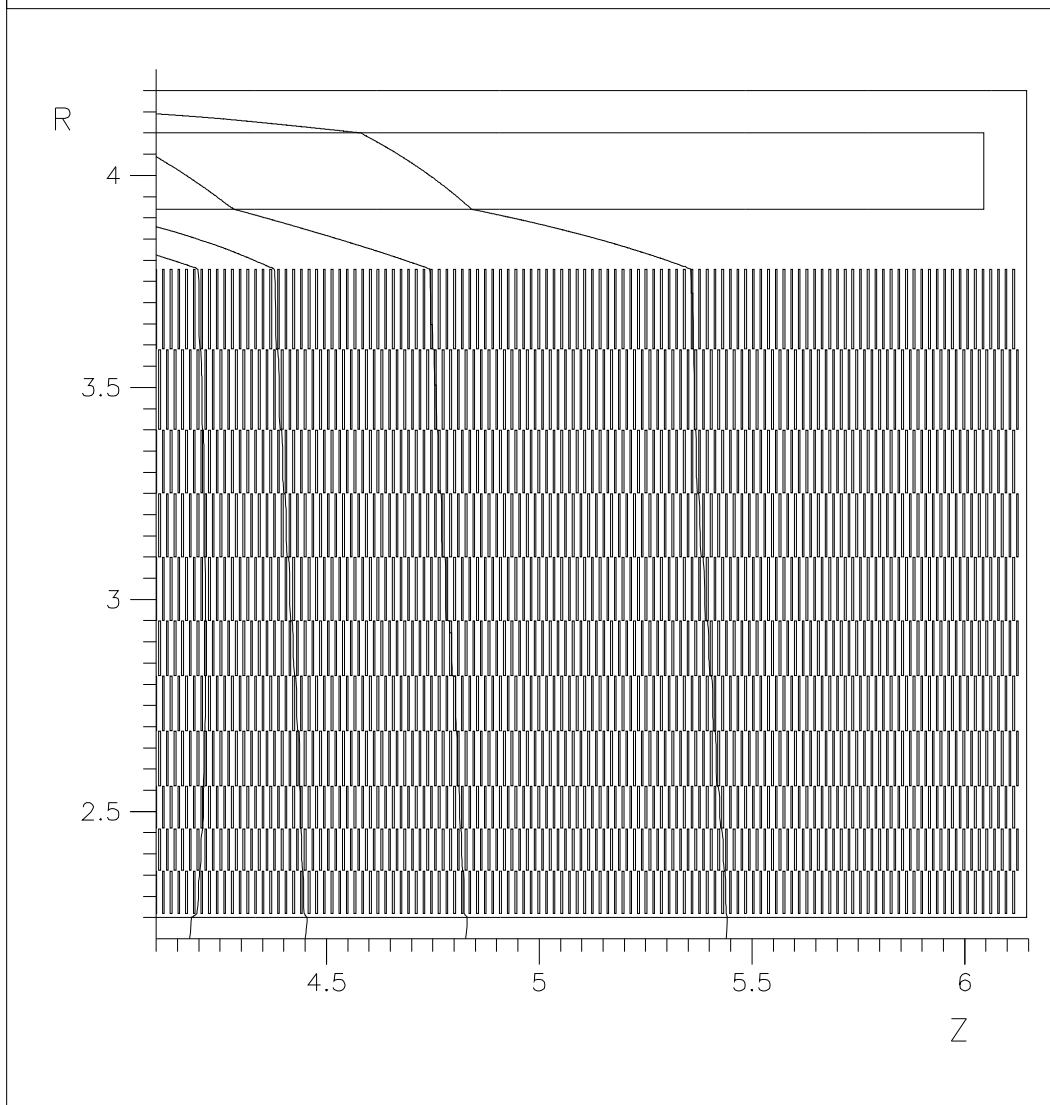


Figure 2-c. Behaviour of the solenoid magnetic field inside the tile calorimeter.

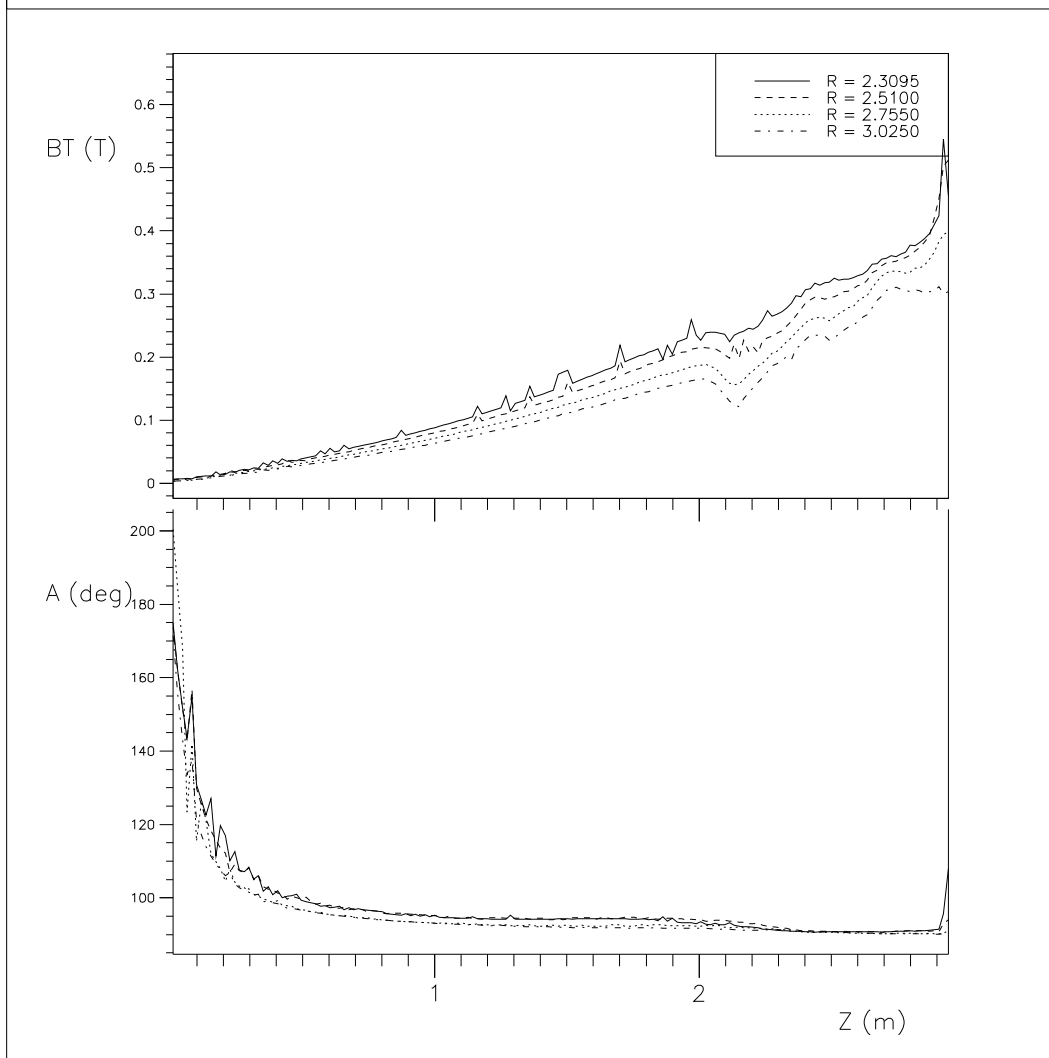


Figure 3. Dependence of total magnetic flux density (upper) and the angle between its vector and z-axis (lower) vs z-coordinate inside steel of the tile calorimeter central barrel for different radii.

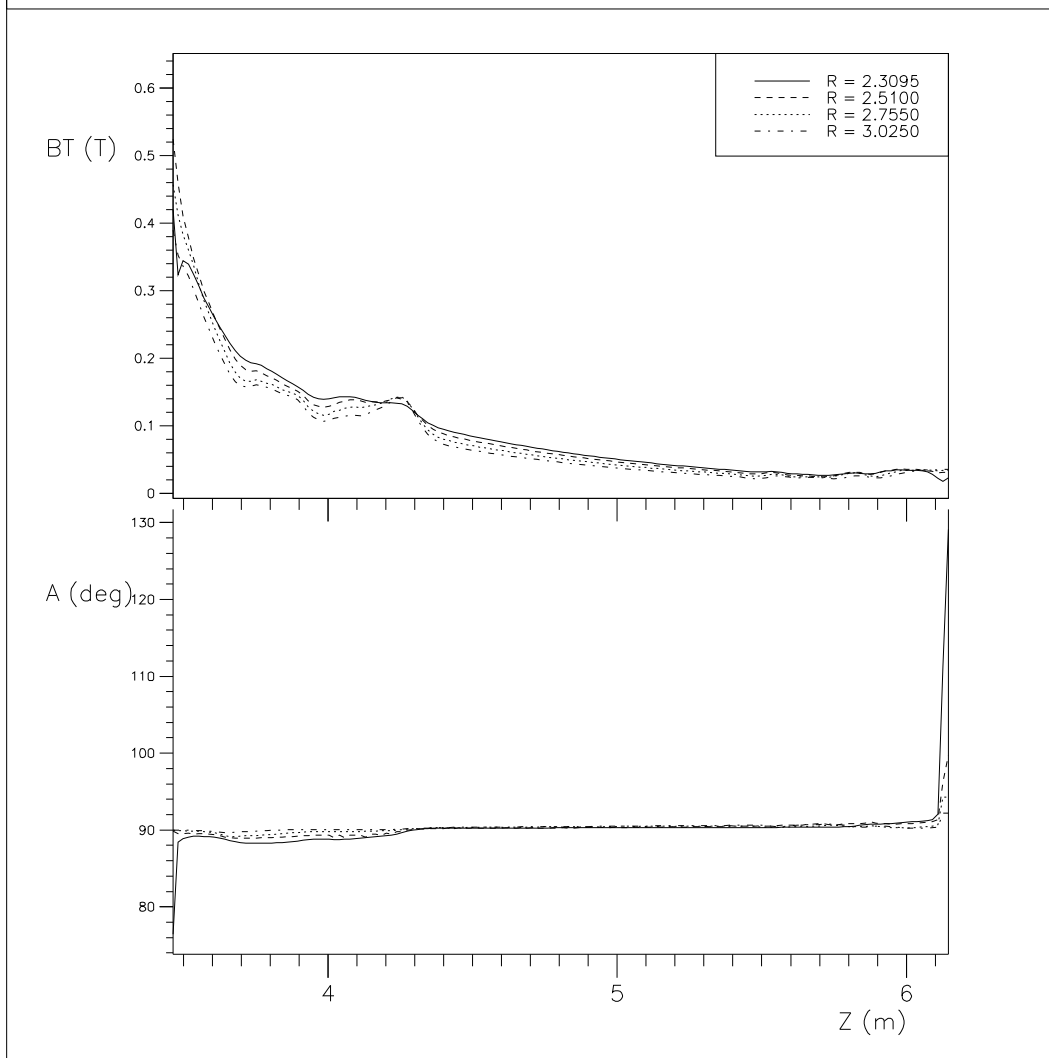


Figure 4. Dependence of total magnetic flux density (upper) and the angle between its vector and z-axis (lower) vs z-coordinate inside steel of the tile calorimeter extended barrel for different radii.

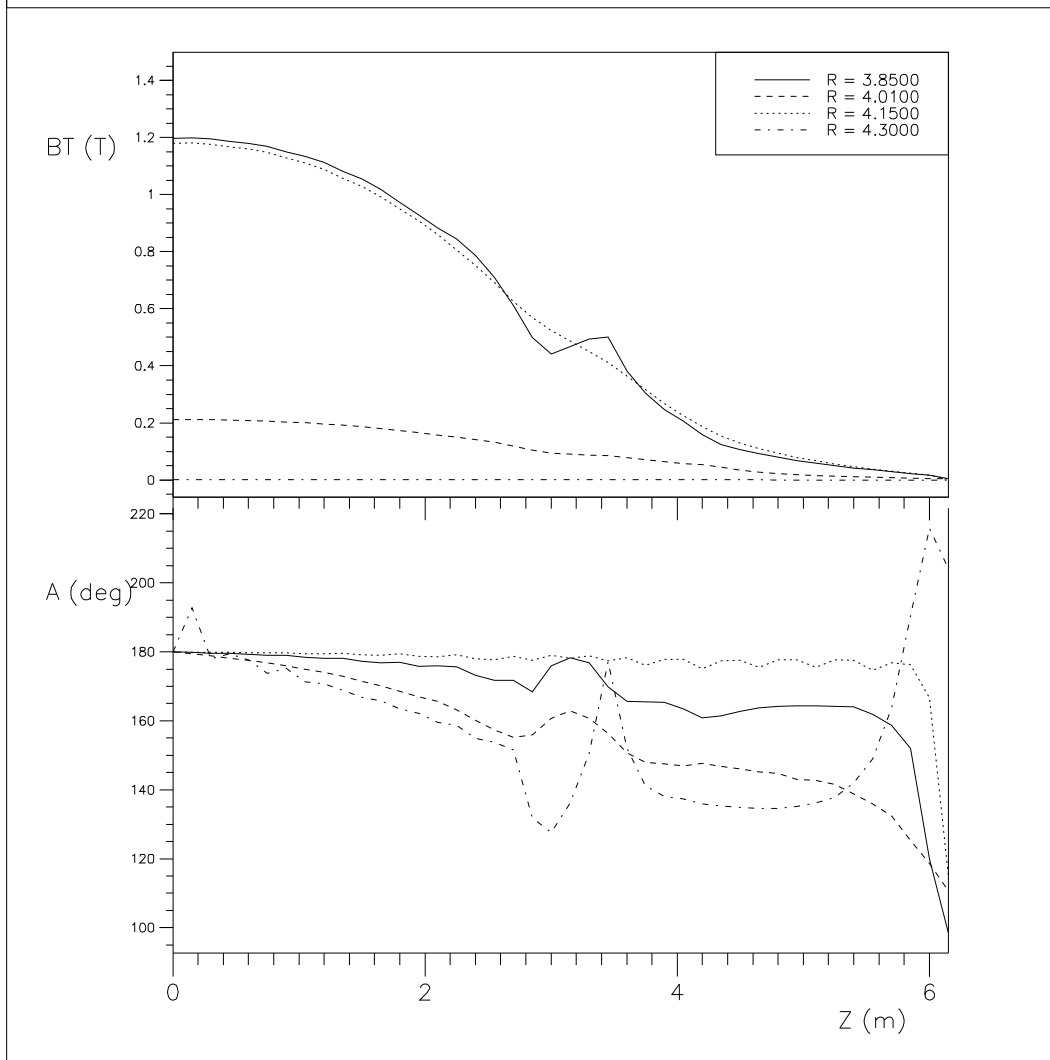


Figure 5. Dependence of total magnetic flux density (upper) and the angle between its vector and z-axis (lower) vs z-coordinate inside and outside the solenoid return yoke for different radii.

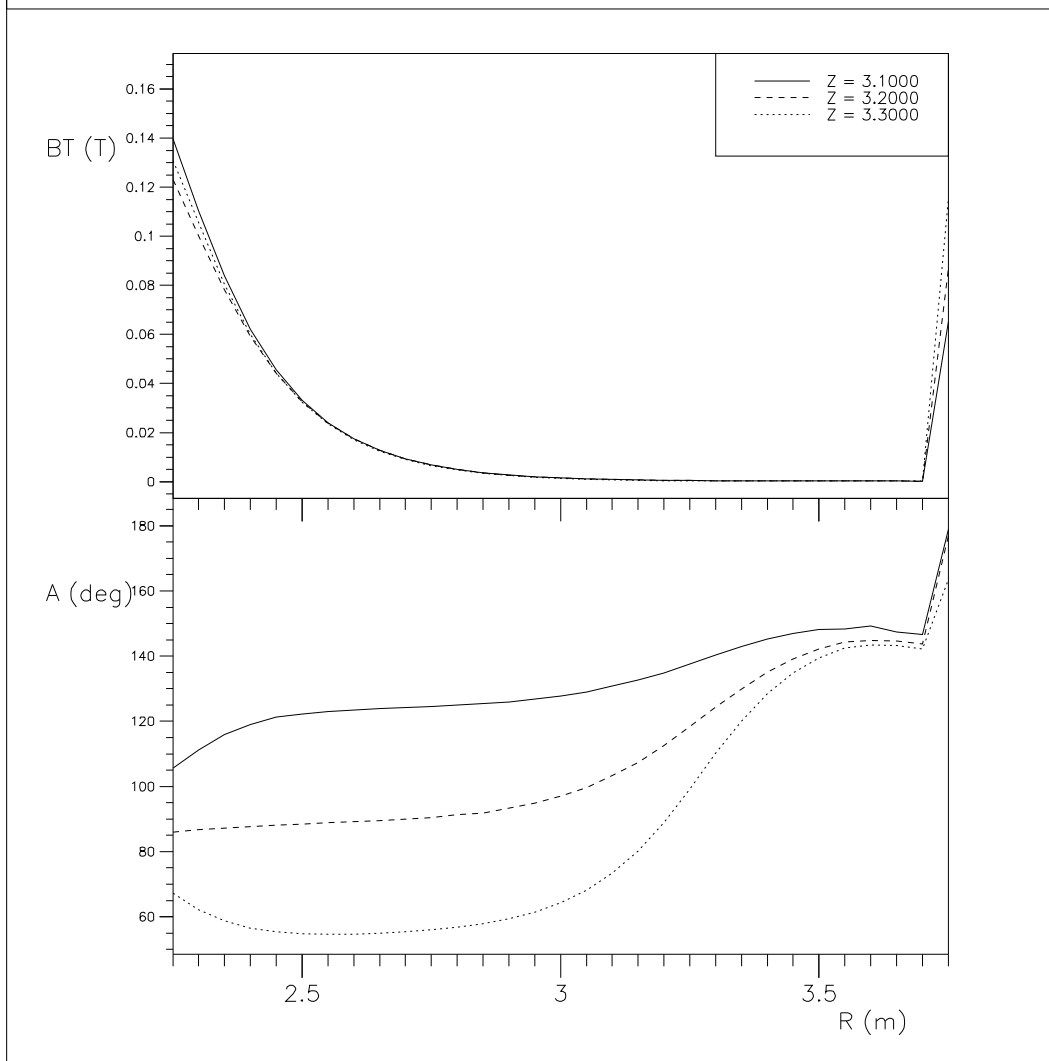


Figure 6. Dependence of total magnetic flux density (upper) and the angle between its vector and  $z$ -axis (lower) vs radius inside crack between central and extended barrels for different  $z$  values.

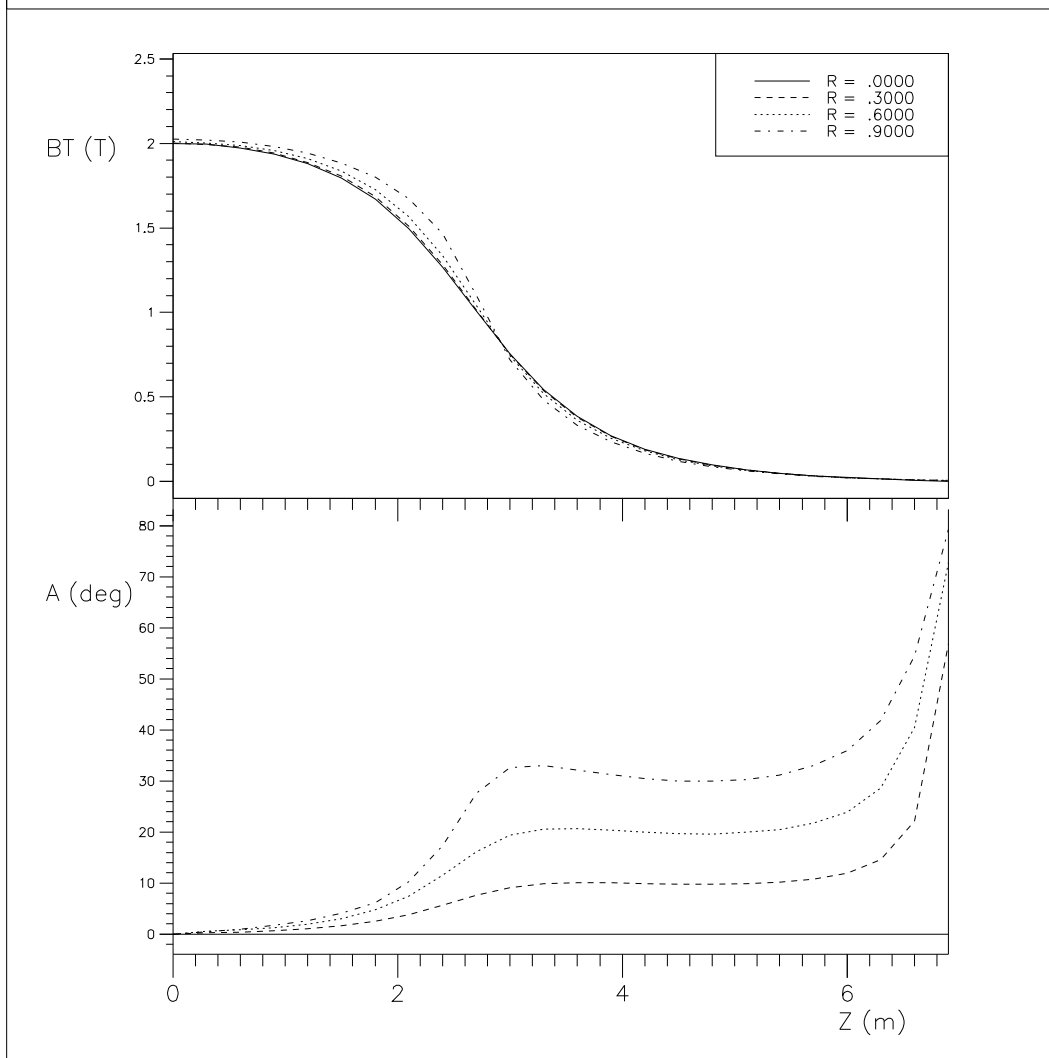


Figure 7. Dependence of total magnetic flux density (upper) and the angle between its vector and z-axis (lower) vs z-coordinate inside the inner tracker cavity for different radii.



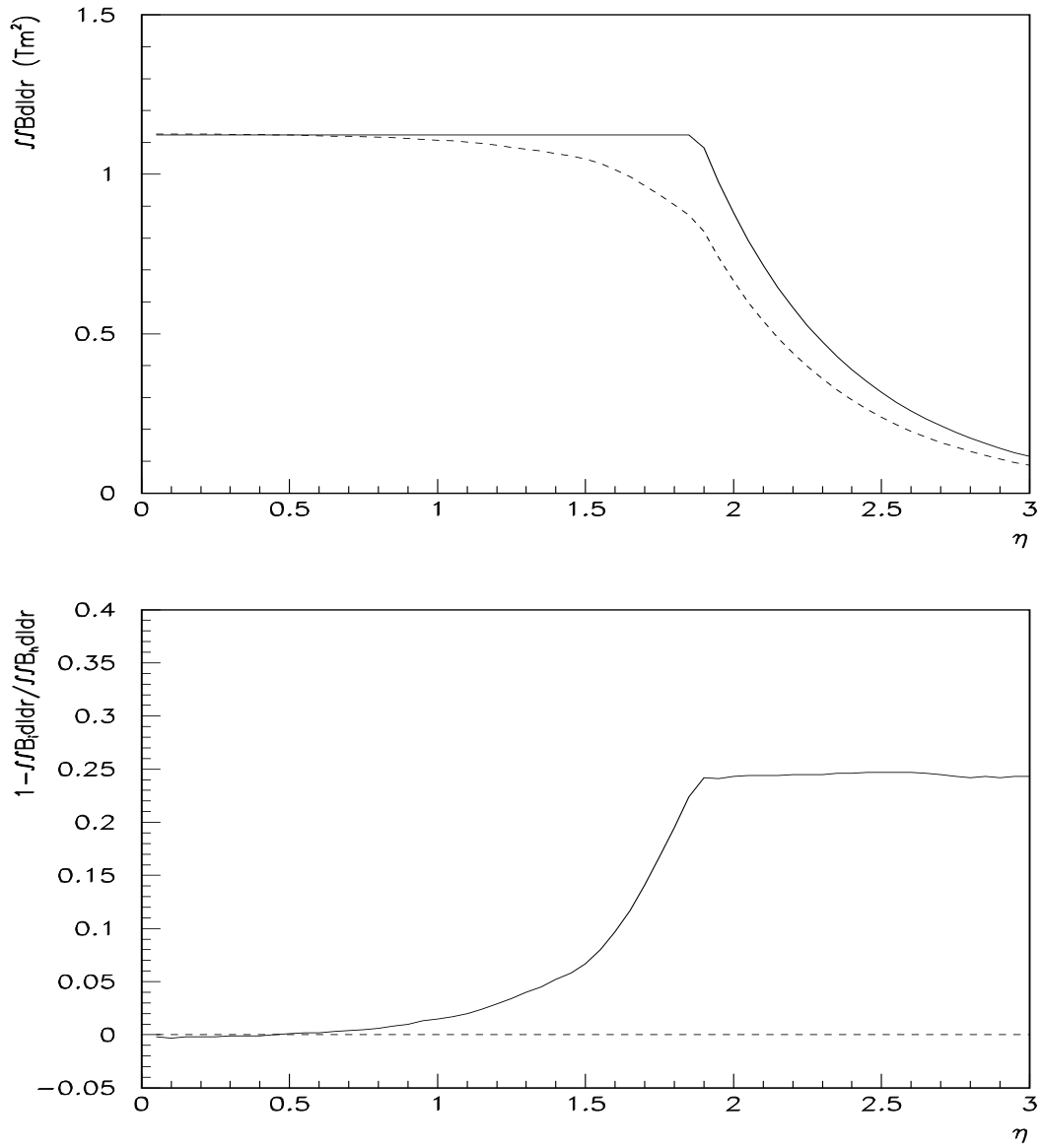


Figure 8. Double integrals calculated inside the inner tracker volume for real (dashed line, upper) and ideal (solid line, upper) solenoid magnetic field and the real integral degradation (solid line, lower).

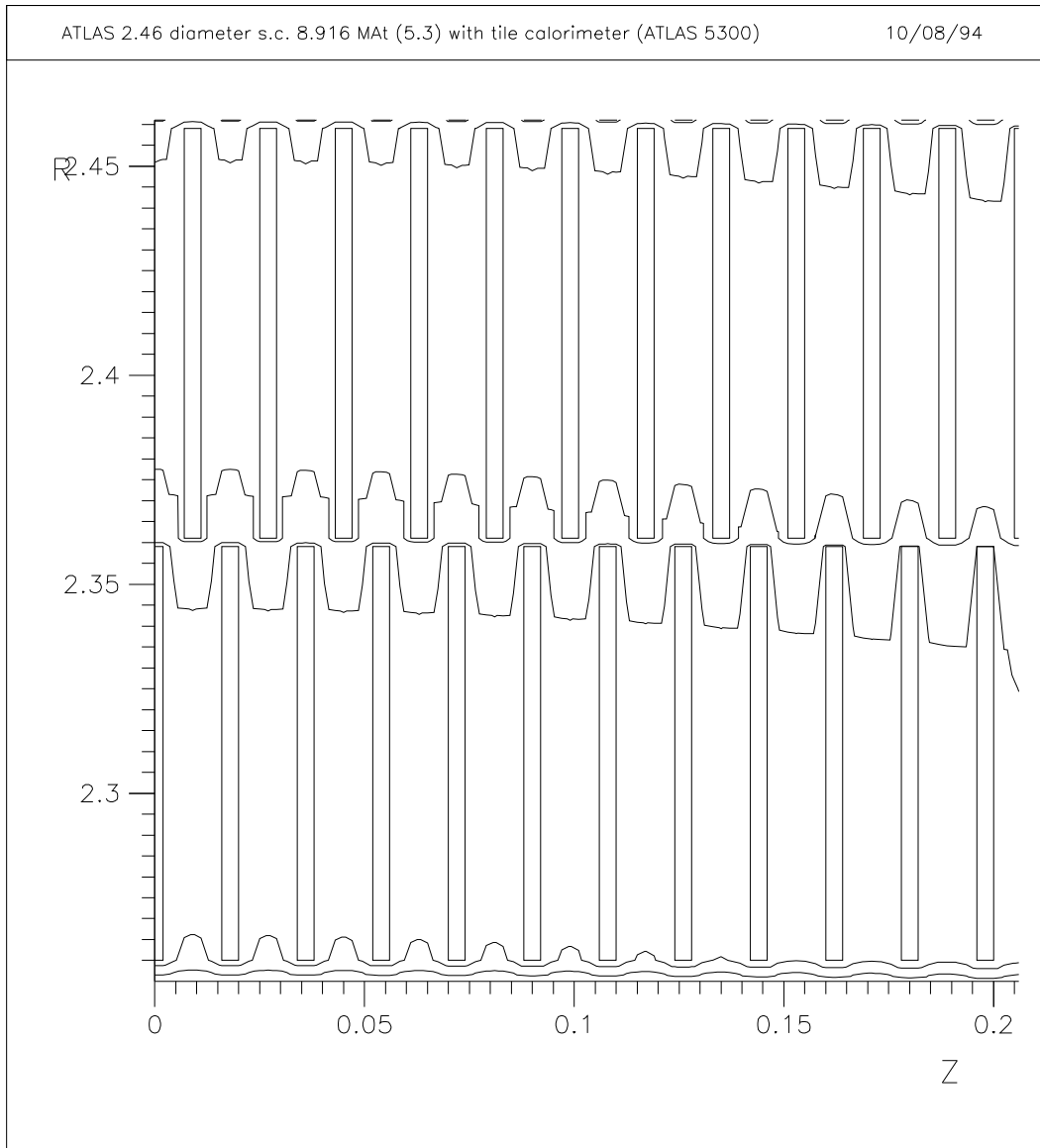


Figure 9. Detail behaviour of the solenoid magnetic field inside the tile calorimeter.

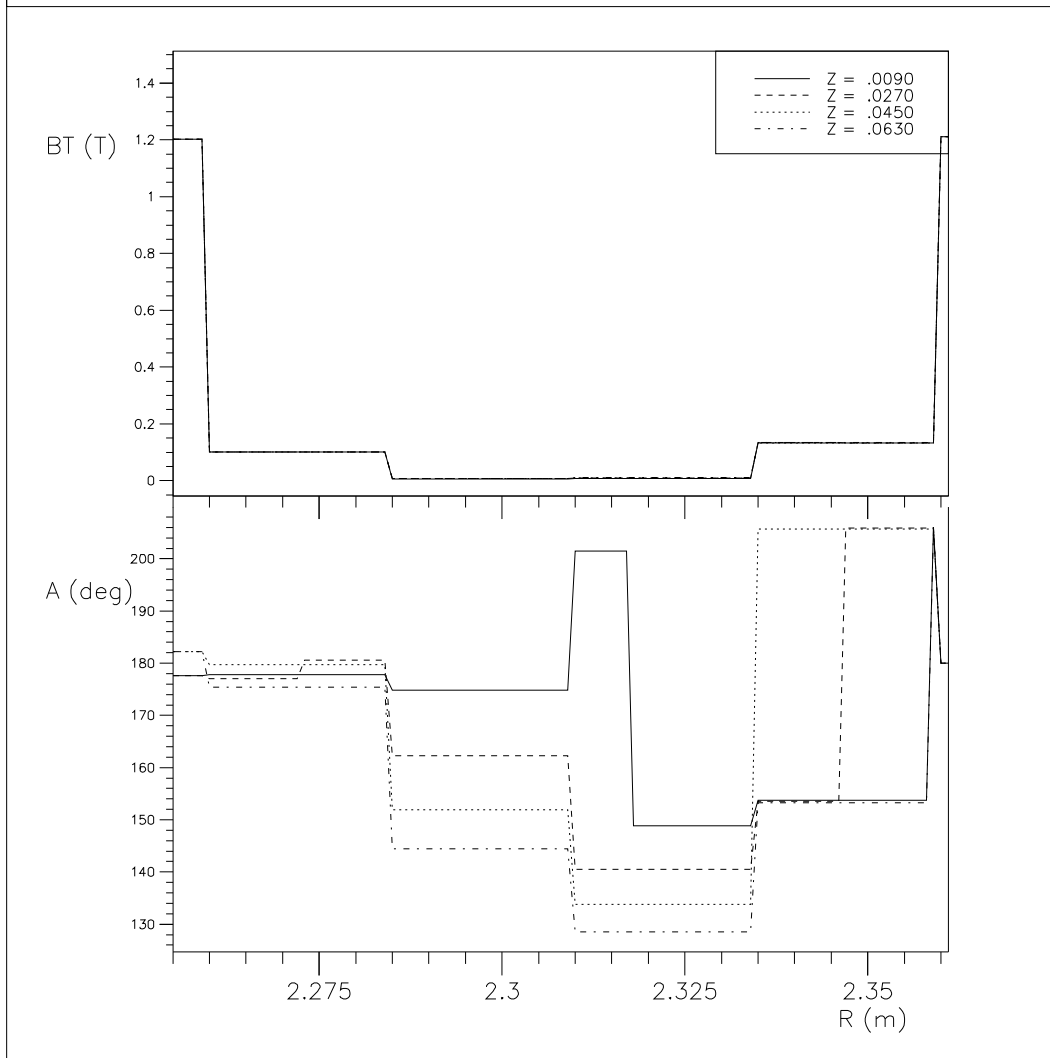


Figure 10. Dependence of total magnetic flux density (upper) and the angle between its vector and z-axis (lower) vs radius inside steel of the tile calorimeter central barrel for different  $z$  values.

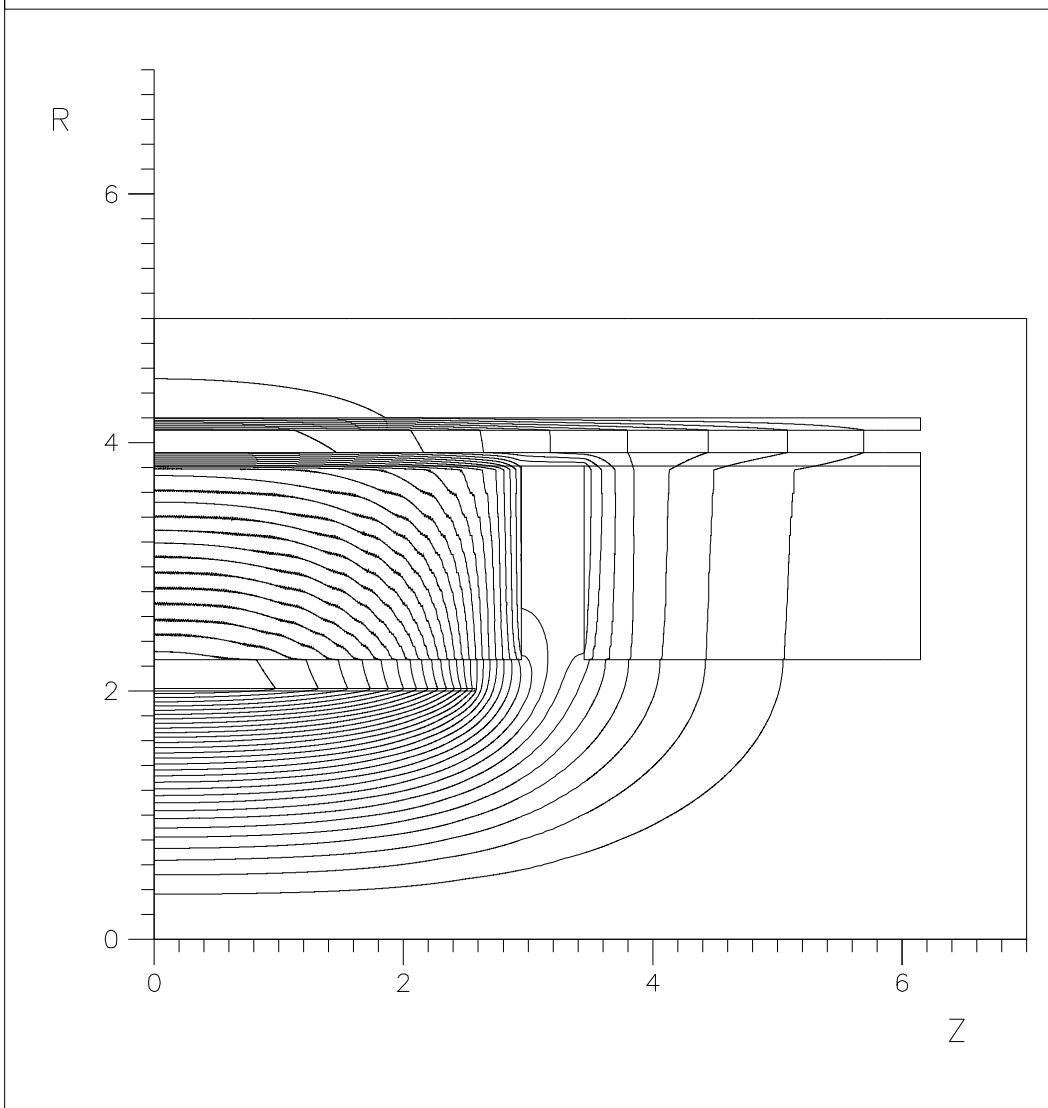


Figure 11. General view of 5.15 m long “large” solenoid magnetic system.

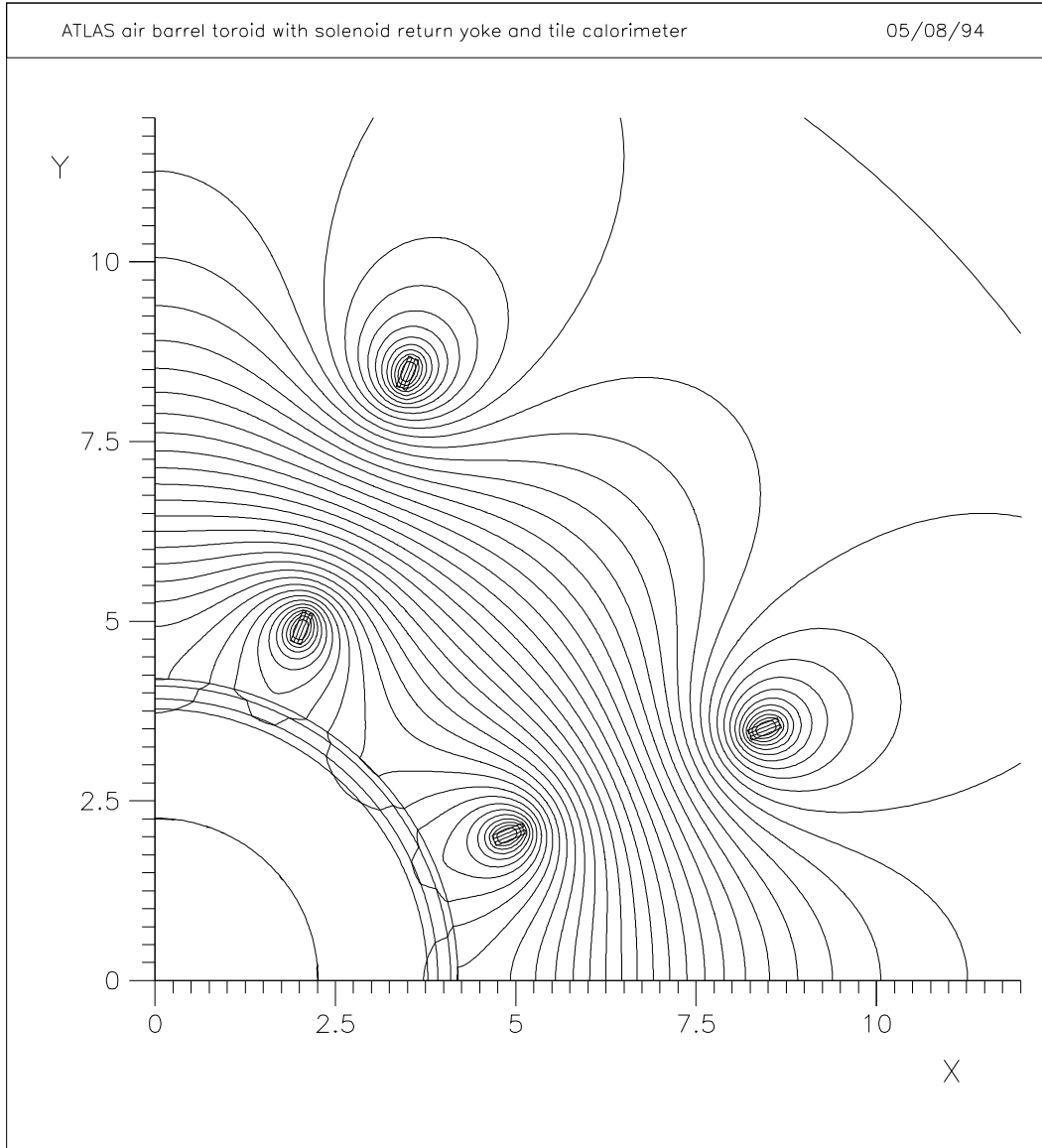


Figure 12. General view of the barrel toroid magnetic system together with the tile calorimeter.

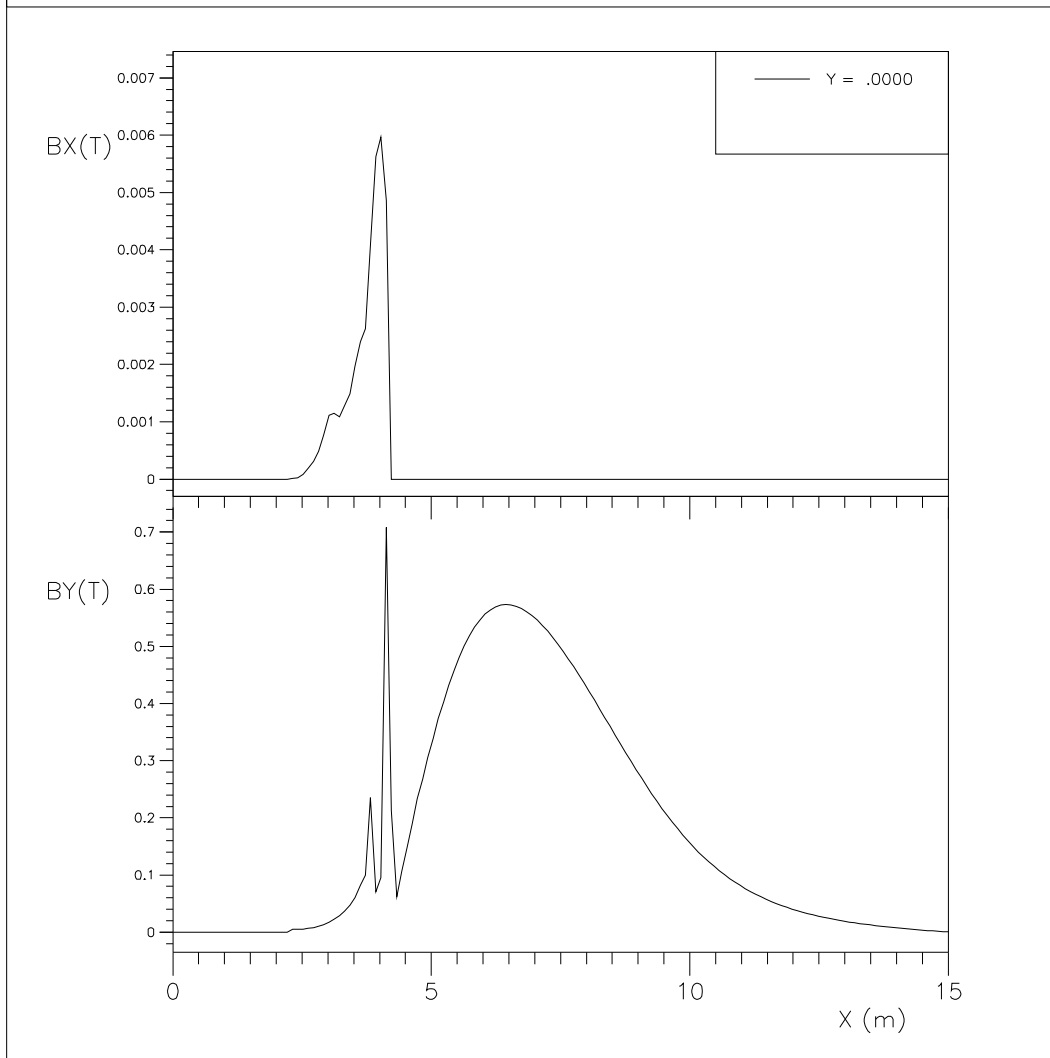


Figure 13. Dependence of radial (upper) and azimuthal (lower) components of the toroid magnetic flux density vs x-coordinate along x-axis.

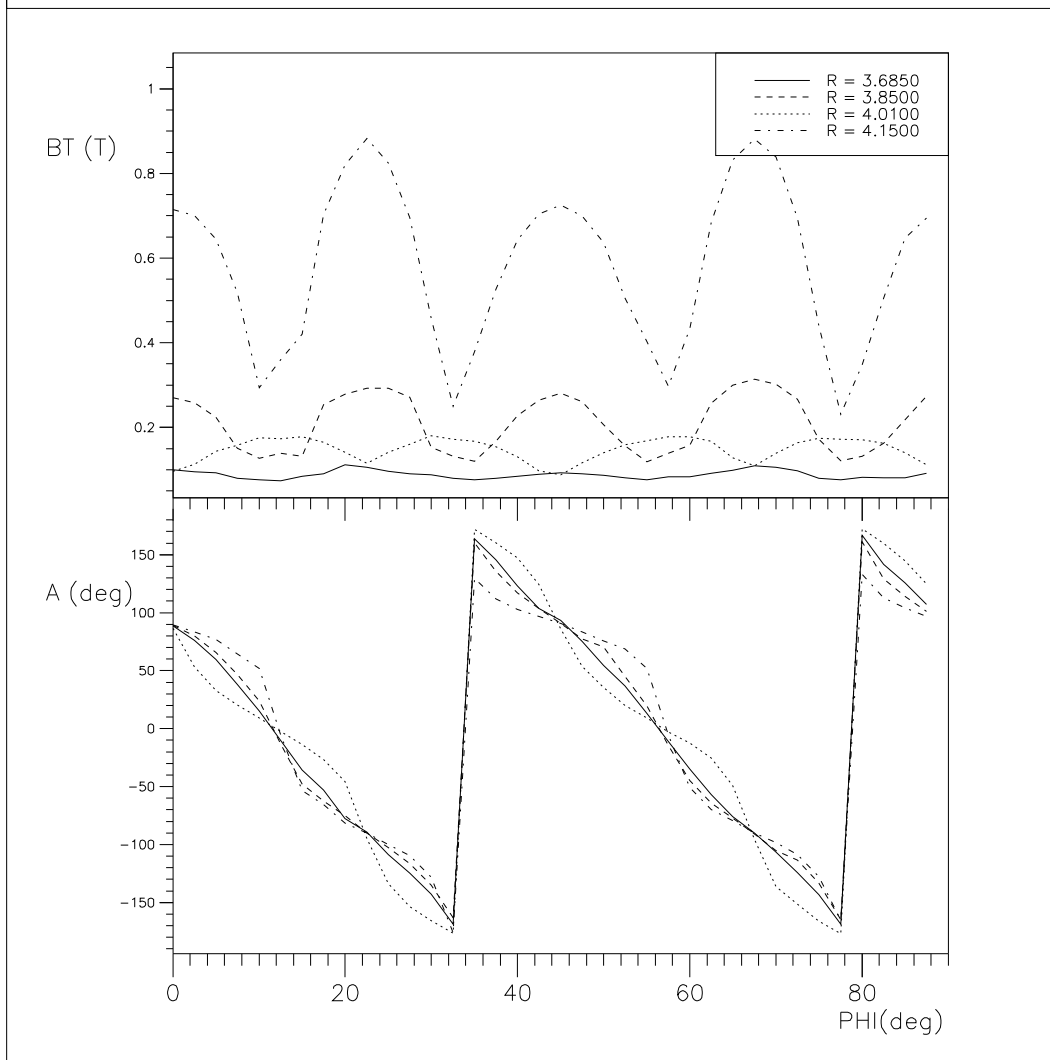


Figure 14. Dependence of the toroid total magnetic flux density (upper) and the angle between its vector and radial direction (lower) vs azimuthal angle inside the tile calorimeter and solenoid return yoke.